

1 **The Spike Protein S1 Subunit of SARS-CoV-2 Contains an LxxIxE-like Motif that is**
2 **Known to Recruit the Host PP2A-B56 Phosphatase**

3

4 Halim Maaroufi

5 Institut de biologie intégrative et des systèmes (IBIS). Université Laval. Quebec. Canada

6 Halim.maaroufi@ibis.ulaval.ca

7

8 **ABSTRACT** The novel betacoronavirus (SARS-CoV-2) is highly contagious and can cause
9 serious acute respiratory illness syndromes, often fatal, called covid-19. It is an urgent priority to
10 better understand SARS-CoV-2 infection mechanisms that will help in the development of
11 prophylactic vaccines and therapeutics that are very important to people health and socioeconomic
12 stability around the world. The surface coronavirus spike (S) glycoprotein is considered as a key
13 factor in host specificity because it mediates infection by receptor-recognition and membrane
14 fusion. Here the analysis of CoV-2 S protein revealed in S1 subunit a B56-binding LxxIxE-like
15 motif that could recruit the host protein phosphatase 2A (PP2A). This motif is absent in SARS-
16 CoV and MERS-CoV. PP2A is a major family of serine/threonine phosphatases in eukaryotic cells.
17 Phosphatases and kinases are big players in the regulation of pro-inflammatory responses during
18 pathogenic infections. Moreover, studies have shown that viruses use multiple strategies to target
19 PP2A in order to manipulate host's antiviral responses. The latest studies have indicated that
20 SARS-CoV-2 is involved in sustained inflammation in the host. Therefore, by controlling acute
21 inflammation; it is possible to eliminate its dangerous effects on the host. Among efforts to fight
22 covid-19, the interaction between LxxIxE-like motif and PP2A-B56-binding pocket could be a
23 target for the development of a bioactive peptide and ligand inhibitors for therapeutic purposes.

24

25

26 **KEYWORDS** Coronavirus; SARS-CoV-2; spike S glycoprotein; PP2A-B56 phosphatase;
27 LxxIxE-like motif; inflammation; therapeutic peptides.

28 INTRODUCTION

29

30 In March 11th 2020, the World Health Organization (WHO) announced that covid-19 situation is a
31 pandemic because of the speed and scale of transmission. Coronaviruses (CoVs) are a large family
32 of enveloped single positive-stranded RNA viruses that can infect both mammalian and avian
33 species because their rapid mutation and recombination facilitate their adaptation to new hosts
34 (Graham and Baric, 2010; Li, 2013). They can cause severe, often fatal acute respiratory disease
35 syndromes named covid-19. CoVs are classified into *Alpha-*, *Beta-*, *Gamma-*, and
36 *Deltacoronavirus* genetic genera. The novel betacoronavirus (betaCoVs) SARS-CoV-2 is
37 relatively close to other betaCoVs: severe acute respiratory syndrome coronavirus (SARS-CoV),
38 Middle East respiratory syndrome coronavirus (MERS-CoV), bat coronavirus HKU4, mouse
39 hepatitis coronavirus (MHV), bovine coronavirus (BCoV), and human OC43 coronavirus (HCoV-
40 OC43). SARS-CoV emerged in China (2002–2003) and spread to other countries (more than 8,000
41 infection cases and a fatality rate of ~10%) (Peiris et al., 2003). In 2012, MERS-CoV was detected
42 in the Middle East. It spread to multiple countries, infecting more than 1,700 people with a fatality
43 rate of ~36%.

44 The surface-located SARS-CoV-2 spike glycoprotein S (S) is a 1273 amino acid residues. It is a
45 homotrimeric, multidomain, and integral membrane protein that give coronaviruses the appearance
46 of having crowns (*Corona* in Latin) (Li, 2016). It is a key piece of viral host recognition (receptor-
47 recognition) and organ tropism and induces strongly the host immune reaction (Li, 2015). It is
48 subdivided to S1 subunit that binds to a receptor on the host cell surface and S2 subunit that permits
49 viral and host membranes fusion. S1 subunit is divided into two domains, an N-terminal domain
50 (NTD) and a C-terminal receptor-binding domain (RBD) that can function as viral receptors-
51 binding (Li, 2012). In addition, S1 subunit is normally more variable in sequence among different
52 CoVs than is the S2 subunit (Masters, 2006).

53 Protein phosphatase 2A (PP2A) is a major family of serine/threonine phosphatases in eukaryotic
54 cells and regulates diverse biological processes through dephosphorylation of numerous signaling
55 molecules. PPA2 and phosphatase 1 (PP1), regulates over 90% of all ser/thr dephosphorylation
56 events in eukaryotic cells (Eichhorn et al., 2009). PP2A is a heterotrimeric holoenzyme composed
57 of a stable heterodimer of the scaffold A-subunit (PP2A-A) and catalytic C-subunit (PP2A-C) and
58 a variable mutually exclusive regulatory subunit from four families (B (B55), B' (B56), B'' and B''')

59 which provide substrate specificity. The human B56 family consists of at least five different
60 members (α , β , γ , δ and ϵ). Phosphatases and kinases are big players in the regulation of pro-
61 inflammatory responses during microbial infections. Moreover, studies have revealed that viruses
62 use multiple strategies to target PP2A in the aim to manipulate host antiviral responses (Guergnon
63 et al., 2011). Here, face to urgent priority to fight the novel SARS-CoV-2 due to its grave
64 consequences in the human health and socioeconomic stability around the world, S protein was
65 analyzed because its importance in mediating infection. This analysis revealed in S1 subunit a B56-
66 binding LxxIxE-like motif that could recruit the host PP2A. The interaction S1 subunit-host PP2A-
67 B56 could be a target for the development of a bioactive peptide and ligand inhibitors for
68 therapeutic purposes.

69

70 **RESULTS AND DISCUSSION**

71

72 *Two LxxIxE-like motifs in S1 and S2 subunits of Spike S*

73

74 Sequence analysis of SARS-CoV-2 spike protein by the eukaryotic linear motif (ELM) resource
75 (<http://elm.eu.org/>) revealed short linear motifs (SLiMs) known as LxxIxE-like motif
76 ,²⁹³LDPLSE²⁹⁸ in S1 subunit and ¹¹⁹⁷LIDLQE¹²⁰² in S2 subunit (Fig. 1). SLiMs are few amino
77 acid residues (3-15) in proteins that facilitate protein sequence modifications and protein-protein
78 interactions (Davey et al., 2012; Van Roey et al., 2014). Viruses are known to mutate quickly and
79 thus create mimic motifs, on very short time scales, that could hijack biological processes in the
80 host cell such as cell signaling networks (Davey et al., 2015; Via et al., 2015; Davey et al., 2011).
81 Interestingly, ²⁹³LDPLSET²⁹⁹ is only present in SARS-CoV-2 (Fig. 1A). It is absent in the other
82 coronaviruses S protein analysed in this study. In order to interact with protein(s), ²⁹³LDPLSE²⁹⁸
83 must be present at the surface of S1 subunit. Indeed, it is exposed in the surface of S1 subunit in
84 the end of NTD (Fig. 3B). Additionally, this motif could be an antigenic epitope to generate
85 antibodies and/or can help the design of vaccine components and immuno-diagnostic reagents. A
86 second motif ¹¹⁹⁷LIDLQEL¹²⁰³ is present in S2 subunit. It is conserved in S2 subunit of SARS-
87 CoV-2, SARS-CoV, SARS-like of bat from China and Kenya (Fig. 1B). These last
88 betacoronaviruses are phylogenetically close (Fig. 2). Unfortunately, the region containing
89 ¹¹⁹⁷LIDLQEL¹²⁰³ peptide has not been resolved in all known structures of spike S protein of
90 coronaviruses to know if it is exposed in the surface of S2 subunit.

91 *Interactions of ²⁹³LDPLSET²⁹⁹ and ¹¹⁹⁷LIDLQEL¹²⁰³ with Subunit B56-PP2A*

92
93 To compare the interactions between these peptides and B56 regulatory subunit of PP2A, molecular
94 docking was performed with the software AutoDock vina (Trott and Olson, 2010). Fig. 4 shows
95 that peptides are localized in the same region as pS-RepoMan peptide (PDBid: 5SW9) and
96 important amino acids of LxxIxE-like motif are superposed with those of pS-RepoMan peptide
97 (Fig. 4C). Interestingly, ²⁹³LDPLSET²⁹⁹ contains a serine and threonine that could be
98 phosphorylated generating a negative charge that will interact with positive patch in subunit B56
99 of PP2A, enhancing binding affinity (Fig. 4A) (Nygren and Scott, 2015). According to Autodock
100 software, binding affinity of ²⁹³LDPLSET²⁹⁹ is -4.8 Kcal/mol and this of ¹¹⁹⁷LIDLQEL¹²⁰³ is -3.5
101 Kcal/mol. The difference of binding affinity may be explained by the phosphorylation of serine and
102 threonine. It is known that the binding affinity of SLiMs is relatively weak (low μmolar range)
103 (Gouw et al., 2018). This knowledge of molecular interactions of ²⁹³LDPLSET²⁹⁹ and B56-PP2A
104 will pave the way to design a peptide able to mimic the surface of B56-PP2A and strongly bind to
105 ²⁹³LDPLSET²⁹⁹ surface precluding PP2A's recruitment (Zaidman and Wolfson, 2016).

106

107 *Protein phosphatase 2A and single RNA viruses*

108
109 It has been shown in single RNA viruses, Ebola virus (EBOV) and Dengue fever virus (DENV)
110 that they recruit the host PP2A through its regulatory subunit B56-binding LxxIxE motif to activate
111 transcription and replication (Kruse et al., 2018; Oliveira et al., 2018). In addition, it has been
112 shown in mice infected with rhinovirus 1B (the most common viral infectious agent in humans) an
113 exacerbation of lung inflammation. Administering Salmeterol (beta-agonist) treatment exerts anti-
114 inflammatory effects by increasing PP2A activity. It is probable that beta-agonists have the
115 potential to target distinct proinflammatory pathways unresponsive to corticosteroids in patients
116 with rhinovirus-induced exacerbations. (Hatchwell et al., 2014). It is interesting to learn about
117 Salmeterol drug and the possibility of using it in covid-19's patients with sustained and dangerous
118 inflammatory reaction.

119 **MATERIALS AND METHODS**

120

121 *Sequence analysis*

122

123 To search probable short linear motifs (SLiMs), SARS-CoV-2 spike protein sequence was
124 scanned with the eukaryotic linear motif (ELM) resource (<http://elm.eu.org/>).

125

126 *3D modeling and molecular docking*

127

128 For docking, the coordinates of the ²⁹³LDPLSET²⁹⁹ peptide were extracted from spike S protein
129 of CoV-2 structure (PDBid: 6VSB_A). Unfortunately, the region containing ¹¹⁹⁷LIDLQEL¹²⁰³
130 peptide has not been resolved in all known structures of spike S protein. So, Pep-Fold (Thevenet
131 et al., 2012) software was used to model *de novo* this peptide. The model quality of the peptide
132 was assessed by analysis of a Ramachandran plot through PROCHECK (Vaguine et al., 1999).
133 The docking of the two peptides into regulatory subunit B56 of PPA2 (PDBid: 5SWF_A) was
134 performed with the software AutoDock vina (Trott and Olson, 2010). The 3D complex
135 containing regulatory subunit B56 of PPA2 and peptides was refined by using FlexPepDock
136 (London et al., 2011), which allows full flexibility to the peptide and side-chain flexibility to the
137 receptor. The electrostatic potential surface of the regulatory subunit B56 of PPA2 was realized
138 with PyMOL software (<http://pymol.org/>).

139

140 *Phylogeny*

141

142 To establish the phylogenetic relationships between spike S protein of SARS-CoV-2 and
143 representative betacoronaviruses, amino acid residues sequences were aligned with Clustal
144 omega (Sievers et al., 2011) and a phylogenetic tree was constructed with MrBayes (Huelsenbeck
145 and Ronquist, 2001) using: Likelihood model (Number of substitution types: 6(GTR);
146 Substitution model: Poisson; Rates variation across sites: Invariable + gamma); Markov Chain
147 Monte Carlo parameters (Number of generations: 100 000; Sample a tree every: 1000
148 generations) and Discard first 500 trees sampled (burnin).

149

150 **ACKNOWLEDGMENTS**

151 I would like to thank the IBIS bioinformatics group for their assistance.

152

153 **CONFLICT OF INTERESTED**

154 The author declares that he has no conflicts of interest.

155

156

157 **REFERENCES**

158 Davey, N.E., Cyert, M.S., Moses, A.M., 2015. Short linear motifs - ex nihilo evolution of protein
159 regulation. *Cell Commun. Signal.* 13, 43. <https://doi.org/10.1186/s12964-015-0120-z>.

160

161 Davey, N.E., Travé, G., Gibson, T.J., 2011. How viruses hijack cell regulation. *Trends Biochem.*
162 *Sci.* 36, 159–169. <https://doi.org/10.1016/j.tibs.2010.10.002>

163

164 Davey, N.E., Van Roey, K., Weatheritt, R.J., Toedt, G., Uyar, B., Altenberg, B., Budd, A.,
165 Diella, F., Dinkel, H., Gibson, T.J., 2012. Attributes of short linear motifs. *Mol. Biosyst.* 8, 268–
166 281. <https://doi.org/10.1039/c1mb05231d>

167

168 Eichhorn, P.J.A., Creighton, M.P., Bernards, R., 2009. Protein phosphatase 2A regulatory
169 subunits and cancer. *Biochim. Biophys. Acta* 1795, 1–15.

170 <https://doi.org/10.1016/j.bbcan.2008.05.005>

171

172 Gouw, M., Michael, S., Sámano-Sánchez, H., Kumar, M., Zeke, A., Lang, B., Bely, B., Chemes,
173 L.B., Davey, N.E., Deng, Z., Diella, F., Gürth, C.-M., Huber, A.-K., Kleinsorg, S., Schlegel, L.S.,
174 Palopoli, N., Roey, K.V., Altenberg, B., Reményi, A., Dinkel, H., Gibson, T.J., 2018. The
175 eukaryotic linear motif resource - 2018 update. *Nucleic Acids Res.* 46, D428–D434.

176 <https://doi.org/10.1093/nar/gkx1077>

177

178 Graham, R.L., Baric, R.S., 2010. Recombination, reservoirs, and the modular spike: mechanisms
179 of coronavirus cross-species transmission. *J. Virol.* 84, 3134–3146.

180 <https://doi.org/10.1128/JVI.01394-09>

181

182 Guernon, J., Godet, A.N., Galioot, A., Falanga, P.B., Colle, J.-H., Cayla, X., Garcia, A., 2011.
183 PP2A targeting by viral proteins: a widespread biological strategy from DNA/RNA tumor viruses
184 to HIV-1. *Biochim. Biophys. Acta* 1812, 1498–1507.

185 <https://doi.org/10.1016/j.bbadis.2011.07.001>

186

187 Hatchwell, L., Girkin, J., Dun, M.D., Morten, M., Verrills, N., Toop, H.D., Morris, J.C.,
188 Johnston, S.L., Foster, P.S., Collison, A., Mattes, J., 2014. Salmeterol attenuates chemotactic
189 responses in rhinovirus-induced exacerbation of allergic airways disease by modulating protein
190 phosphatase 2A. *J. Allergy Clin. Immunol.* 133, 1720–1727.

191 <https://doi.org/10.1016/j.jaci.2013.11.014>

192

193 Huelsenbeck, J.P., Ronquist, F., 2001. MRBAYES: Bayesian inference of phylogenetic trees.
194 *Bioinformatics* 17, 754–755. <https://doi.org/10.1093/bioinformatics/17.8.754>

- 195
196 Kruse, T., Biedenkopf, N., Hertz, E.P.T., Dietzel, E., Stalman, G., López-Méndez, B., Davey,
197 N.E., Nilsson, J., Becker, S., 2018. The Ebola Virus Nucleoprotein Recruits the Host PP2A-B56
198 Phosphatase to Activate Transcriptional Support Activity of VP30. *Mol. Cell* 69, 136–145.e6.
199 <https://doi.org/10.1016/j.molcel.2017.11.034>
200
201 Li, F., 2016. Structure, Function, and Evolution of Coronavirus Spike Proteins. *Annu Rev Virol*
202 3, 237–261. <https://doi.org/10.1146/annurev-virology-110615-042301>
203 Li, F., 2015. Receptor recognition mechanisms of coronaviruses: a decade of structural studies. *J.*
204 *Virol.* 89, 1954–1964. <https://doi.org/10.1128/JVI.02615-14>
205
206 Li, F., 2013. Receptor recognition and cross-species infections of SARS coronavirus. *Antiviral*
207 *Res.* 100, 246–254. <https://doi.org/10.1016/j.antiviral.2013.08.014>
208
209 Li, F., 2012. Evidence for a common evolutionary origin of coronavirus spike protein receptor-
210 binding subunits. *J. Virol.* 86, 2856–2858. <https://doi.org/10.1128/JVI.06882-11>
211
212 London, N., Raveh, B., Cohen, E., Fathi, G., Schueler-Furman, O., 2011. Rosetta FlexPepDock
213 web server--high resolution modeling of peptide-protein interactions. *Nucleic Acids Res.* 39,
214 W249–53. <https://doi.org/10.1093/nar/gkr431>
215
216 Masters, P.S., 2006. The molecular biology of coronaviruses. *Adv. Virus Res.* 66, 193–292.
217 [https://doi.org/10.1016/S0065-3527\(06\)66005-3](https://doi.org/10.1016/S0065-3527(06)66005-3)
218
219 Nygren, P.J., Scott, J.D., 2015. Therapeutic strategies for anchored kinases and phosphatases:
220 exploiting short linear motifs and intrinsic disorder. *Front. Pharmacol.* 6, 158.
221 <https://doi.org/10.3389/fphar.2015.00158>
222
223 Oliveira, M., Lert-Itthiporn, W., Cavadas, B., Fernandes, V., Chuansumrit, A., Anunciação, O.,
224 Casademont, I., Koeth, F., Penova, M., Tangnaratchakit, K., Khor, C.C., Paul, R., Malasit, P.,
225 Matsuda, F., Simon-Lorière, E., Suriyaphol, P., Pereira, L., Sakuntabhai, A., 2018. Joint ancestry
226 and association test indicate two distinct pathogenic pathways involved in classical dengue fever
227 and dengue shock syndrome. *PLoS Negl. Trop. Dis.* 12, e0006202.
228 <https://doi.org/10.1371/journal.pntd.0006202>
229
230 Peiris, J.S.M., Lai, S.T., Poon, L.L.M., Guan, Y., Yam, L.Y.C., Lim, W., Nicholls, J., Yee,
231 W.K.S., Yan, W.W., Cheung, M.T., Cheng, V.C.C., Chan, K.H., Tsang, D.N.C., Yung, R.W.H.,
232 Ng, T.K., Yuen, K.Y., SARS study group, 2003. Coronavirus as a possible cause of severe acute
233 respiratory syndrome. *Lancet* 361, 1319–1325. [https://doi.org/10.1016/s0140-6736\(03\)13077-2](https://doi.org/10.1016/s0140-6736(03)13077-2)
234
235 Sievers, F., Wilm, A., Dineen, D., Gibson, T.J., Karplus, K., Li, W., Lopez, R., McWilliam, H.,
236 Remmert, M., Söding, J., Thompson, J.D., Higgins, D.G., 2011. Fast, scalable generation of high-
237 quality protein multiple sequence alignments using Clustal Omega. *Mol. Syst. Biol.* 7, 539.
238 <https://doi.org/10.1038/msb.2011.75>
239
240 Thévenet, P., Shen, Y., Maupetit, J., Guyon, F., Derreumaux, P., Tufféry, P., 2012. PEP-FOLD:

241 an updated de novo structure prediction server for both linear and disulfide bonded cyclic
242 peptides. *Nucleic Acids Res.* 40, W288–93. <https://doi.org/10.1093/nar/gks419>
243
244 Trott, O., Olson, A.J., 2010. AutoDock Vina: improving the speed and accuracy of docking with
245 a new scoring function, efficient optimization, and multithreading. *J. Comput. Chem.* 31, 455–
246 461. <https://doi.org/10.1002/jcc.21334>
247
248 Vaguine, A.A., Richelle, J., Wodak, S.J., 1999. SFCHECK: a unified set of procedures for
249 evaluating the quality of macromolecular structure-factor data and their agreement with the
250 atomic model. *Acta Crystallogr. D Biol. Crystallogr.* 55, 191–205.
251 <https://doi.org/10.1107/S0907444998006684>
252
253 Van Roey, K., Uyar, B., Weatheritt, R.J., Dinkel, H., Seiler, M., Budd, A., Gibson, T.J., Davey,
254 N.E., 2014. Short linear motifs: ubiquitous and functionally diverse protein interaction modules
255 directing cell regulation. *Chem. Rev.* 114, 6733–6778. <https://doi.org/10.1021/cr400585q>
256
257 Via, A., Uyar, B., Brun, C., Zanzoni, A., 2015. How pathogens use linear motifs to perturb host
258 cell networks. *Trends Biochem. Sci.* 40, 36–48. <https://doi.org/10.1016/j.tibs.2014.11.001>
259
260 Wang, X., Bajaj, R., Bollen, M., Peti, W., Page, R., 2016. Expanding the PP2A Interactome by
261 Defining a B56-Specific SLiM. *Structure* 24, 2174–2181.
262 <https://doi.org/10.1016/j.str.2016.09.010>
263
264 Zaidman, D., Wolfson, H.J., 2016. PinaColada: peptide–inhibitor ant colony ad-hoc design
265 algorithm. *Bioinformatics* 32, 2289–2296. <https://doi.org/10.1093/bioinformatics/btw133>
266

267 **Figures**

268

269 **Figure 1.** Multiple alignment of the spike glycoprotein of betacoronaviruses using Clustal omega
270 (Sievers et al., 2011). LxxIxE-like motifs are indicated by green stars. Numbers at the start of
271 each sequence corresponding to the GenBank and UniProt accession number. Green stars
272 indicated LxxIxE-like motif. The figure was prepared with ESPrpt (<http://esprpt.ibcp.fr>).

273

274 **Figure 2.** Unrooted phylogenetic tree of spike protein of representative betacoronaviruses. The
275 tree was constructed using Mr Bayes method (Huelsenbeck and Ronquist, 2001) based on the
276 multiple sequence alignment by Clustal omega (Sievers et al., 2011). Numbers at the start of each
277 sequence corresponding to the GenBank and UniProt accession number. Red rectangle assembles
278 betacoronaviruses with the same ¹¹⁹⁷LIDLQE¹²⁰². Green star indicated the only betacoronavirus
279 with ²⁹³LDPLSE²⁹⁸.

280

281 **Figure 3.** (A) Diagram representation of the S1 subunit of spike protein of SARS-CoV-2 colored
282 by domain. N-terminal domain (NTD, cyan), receptor-binding domain (RBD, green), subdomains
283 1 and 2 (SD1-2, orange) and the localization of ²⁹³LDPLSE²⁹⁸ in the end of NTD.
284 (B) Surface structure representation of the S1 subunit of spike protein (PDBid: 6VSB_A).
285 ²⁹³LDPLSE²⁹⁸ peptide is localized in the surface (red).

286

287 **Figure 4.** Electrostatic potential surface representation of the region of the regulatory subunit
288 B56 of PP2A (PDBid: 5SWF_A) with docked peptides. (A) ²⁹³LDPLpSEpT²⁹⁹ (green), (B)
289 ¹¹⁹⁷LIDLQEL¹²⁰³ (cyan) and (C) ²⁹³LDPLpSEpT²⁹⁹ superposed to pS-RepoMan
290 (⁵⁸¹RDIASKKPLLpSPIPELPEVPE⁶⁰¹) peptide (orange, PDBid: 5SW9_B). The surfaces are colored
291 by electrostatic potential with negative charge shown in red and positive charge in blue. Images
292 were generated using PyMol (www.pymol.org).

293

294

A

| | | | | | | |
|--|----------|--------|-----------|----------|----------|---------|
| | 270 | 280 | 290 | 300 | 310 | 320 |
| YP_009724390.1_Human_SARS-CoV-2_Wuhan-Hu-1_China | VGYIQPR | TFLLKY | NENCTITD | AVDCALDP | LSETKCT | LKSF |
| P59594.1_Human_SARS-Cov_HongKong_China | VGYLKPT | TFMLKY | DENCTITD | AVDCSQNP | LAEKCSVK | SFEIDK |
| ATO98205.1_Bat_SARS-like_coronavirus_China | VGYLKPA | TFMLKY | DENCTITD | AVDCSQNP | LAEKCSVK | SFEIDK |
| APO40579.1_Bat_SARS-like_coronavirus_Kenya | VGHLLKPL | TMLAEF | DENCTITD | AVDCSQDP | LSEIKCT | TKSLT |
| P36334_Human_SPIKE_CVHOC_coronavirus_OC43 | VTFLLTSR | QYLLAF | NQDCIIFNA | EDCMSDF | MSEIKCK | TQSIAP |
| P25190_Bovine_SPIKE_CVBF_coronavirus_strain_F15 | VTFLLTSR | QYLLAF | NQDCIIFNA | EDCMSDF | MSEIKCK | TQSIAP |
| P11225_Murine_SPIKE_CVMJH_coronavirus_JHM | VTFLLTSR | QYLLAF | NQDCIIFNA | EDCMSDF | MSEIKCK | TQSIAP |
| ALK80251.1_Human_MERS-CoV_South-Korea | VYKLLQPL | TFLLDF | SVDGYIRRA | ADCGFND | LSQLHCS | YSYEF |
| A3EX94_Bat_SPIKE_BCHK4_coronavirus_HKU4 | VYKLLQPL | TFLLDF | SVDGYIRRA | ADCGFND | LSQLHCS | YSYEF |
| QGA70702.1_Erinaceus_coronavirus_HKU31_China | TYQLHKL | NYLVEF | DVGCYIVRA | SDCGANDY | TQLQCS | YGFDMNS |

295

296

B

| | | | | | | |
|--|--------|-------|--------|--------|--------|---------|
| | 1190 | 1200 | 1210 | 1220 | 1230 | 1240 |
| YP_009724390.1_Human_SARS-CoV-2_Wuhan-Hu-1_China | NEVAKN | LNESL | IDLQEL | GKYEQY | IKWPWY | IWDGFI |
| P59594.1_Human_SARS-Cov_HongKong_China | NEVAKN | LNESL | IDLQEL | GKYEQY | IKWPWY | VWDLGFI |
| ATO98205.1_Bat_SARS-like_coronavirus_China | NEVAKN | LNESL | IDLQEL | GKYEQY | IKWPWY | VWDLGFI |
| APO40579.1_Bat_SARS-like_coronavirus_Kenya | NEIAKN | LNESL | IDLQEL | GKYEQY | VKWPWY | VWDLGFI |
| P36334_Human_SPIKE_CVHOC_coronavirus_OC43 | QEAIKV | LNQSY | INLKD | IGTYEY | VKWPWY | VWDLGFI |
| P25190_Bovine_SPIKE_CVBF_coronavirus_strain_F15 | QEAIKV | LNQSY | INLKD | IGTYEY | VKWPWY | VWDLGFI |
| P11225_Murine_SPIKE_CVMJH_coronavirus_JHM | QEAIKV | LNQSY | INLKD | IGTYEY | VKWPWY | VWDLGFI |
| ALK80251.1_Human_MERS-CoV_South-Korea | QQVVK | LNESY | IDLKEL | GNITYY | NKWPWY | IWDGFI |
| A3EX94_Bat_SPIKE_BCHK4_coronavirus_HKU4 | QEVVK | LNDSY | IDLKEL | GNITYY | NKWPWY | VWDLGFI |
| QGA70702.1_Erinaceus_coronavirus_HKU31_China | QSVVEA | LNQSY | LELKE | LGNYTY | NKWPWY | VWDLGFI |

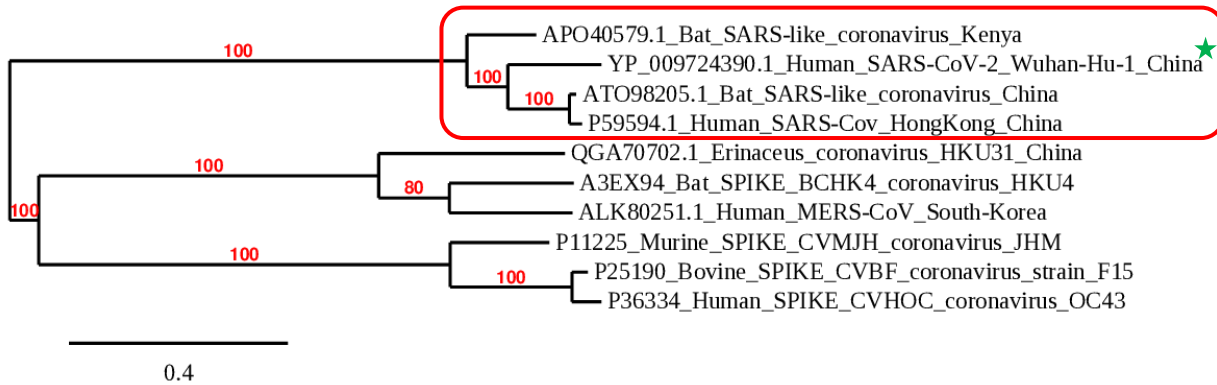
297

298 **Fig. 1**

299

300

1197 **LIDLQEL** 1203



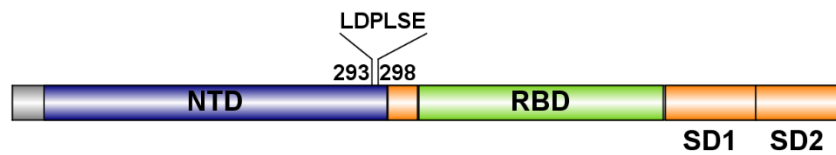
301

302 **Fig. 2**

303

304

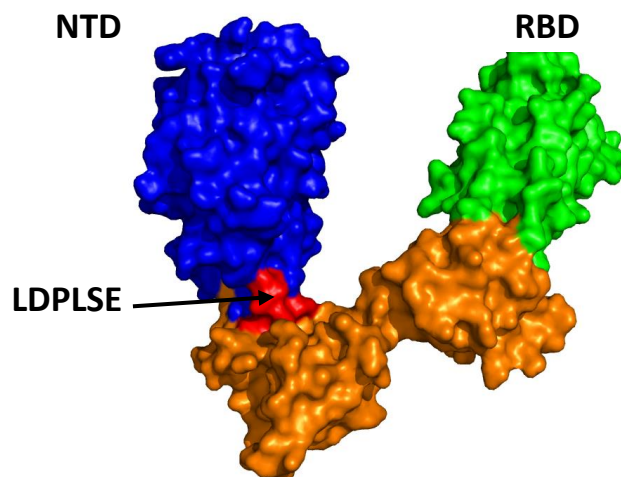
A



305

306

B

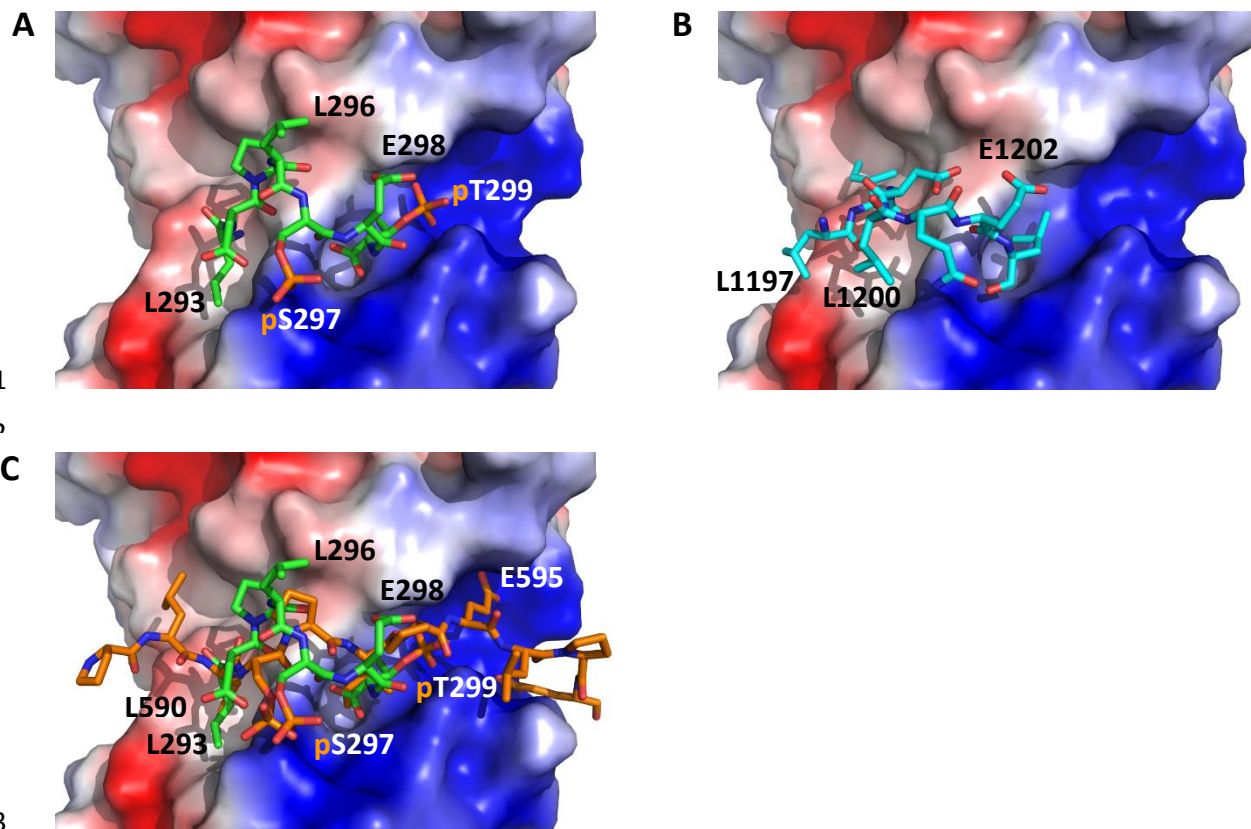


307

308 **Fig. 3**

309

310



315 **Fig. 4**